DEVELOPMENT OF NEW CRITERIA FOR ASSESSING THE RISK OF KNEE-THIGH-HIP INJURY IN FRONTAL IMPACTS USING HYBRID III FEMUR FORCE MEASUREMENTS

Jonathan D. Rupp[1,2], Matthew P. Reed[1,4], Carl S. Miller[1], Nathaniel H. Madura[1], Kathleen D. Klinich, Shashi M. Kuppa[5], and Lawrence W. Schneider[1,3]

[1]University of Michigan Transportation Research Institute (UMTRI)

[2]The University of Michigan, Department of Emergency Medicine

[3]The University Michigan, Department of Biomedical Engineering

[4]The University Michigan, Department of Industrial and Operations Engineering

[5]National Highway Traffic Safety Administration

United States

Paper 09-0306

ABSTRACT

Injury patterns in real-world frontal crashes and the forces predicted in computational simulations of knee impacts suggest that the risk of hip injury is higher than the risk of knee/distal femur injury in most frontal crashes that are similar in severity to those used in FMVSS 208 and NCAP. However, the knee-thigh-hip (KTH) injury criterion that is currently used with Hybrid III femur forces in FMVSS 208 and NCAP only assesses the risk of knee/distal femur injury.

As a first step to developing new KTH injury assessment criteria that apply to hip and knee/distal femur injury, a one-dimensional lumped-parameter model of the Hybrid III ATD was developed and validated. Simulations were performed with this model and a previously validated lumped-parameter model of the cadaver to explore relationships between peak force at the Hybrid III femur load cell and peak force at the cadaver hip over the range of knee-loading conditions that occur in FMVSS 208 and NCAP crash tests. Results of these simulations indicate that there is not a singular relationship between peak Hybrid III femur force and peak force at the cadaver hip or at the knee/distal femur.

Because of the complex relationship between femur force measured in the Hybrid III femur load cells and forces and injury risks in the human KTH, a new injury assessment criterion has been developed for the KTH that uses peak force and impulse calculated from force histories measured by the Hybrid III load cell to determine if the probability of KTH injury exceeds a specified value. The use of impulse allows the new injury assessment criterion to identify the high-rate, short duration loading conditions that are likely to produce knee/distal femur fractures and the slower loading rates and longer durations that are more likely to produce hip fracture/dislocation.

INTRODUCTION

Fractures and dislocations (i.e., AIS 2+ injuries) to the knee-thigh-hip (KTH) complex occur in 2% to 3% of all tow-away frontal crashes of airbag-equipped vehicles (Kirk and Kuppa, 2009) and occur at a rate of approximately 30,000 per year in the US. (Rupp et al. 2002). Of these injuries, approximately 60% are to the shaft of the femur and hip (Kuppa and Kirk, 2009). Although a high proportion of KTH injuries are to the hip and femoral shaft, the risk curve used to establish the current 10-kN maximum femur force injury assessment reference value (IARV) used in FMVSS 208 and NCAP is based on a risk curve that was developed from fracture force data that are almost exclusively associated with knee and distal femur injuries (Rupp et al. 2002, Rupp 2006).

As part of a research program aimed at addressing this shortcoming, previous studies measured the force required to produce fracture of the human cadaver hip under knee-bolster-like loading conditions (Rupp et al. 2002 and 2003, Rupp 2006). Hip fracture force data from these tests were statistically analyzed to develop a new risk curve that expresses the probability of hip fracture as a function of force transmitted to the hip while accounting for stature and lower-extremity posture (Rupp 2008, Rupp et al. 2009). An earlier version of this risk curve was used along with the knee/distal femur injury risk curve reported by Kuppa et al. (2001) in a series of simulations with lumped parameter and finite element models of the KTH complex (Rupp et al., 2008, Chang et al. 2008). Results of these simulations predict that the hip is the part of the KTH complex that is most likely to be injured in a frontal crash for symmetric knee loading and in the absence of muscle tension.

Development of improved IARVs from these KTH injury risk curves is challenging because risk curves are based on fracture forces measured in testing of cadavers, while IARVs must apply to femur forces measured by the Hybrid III family of crash-test dummies. Specifically, results of previous studies demonstrate that the Hybrid III can produce

substantially higher knee impact forces than a similar sized cadaver and that forces at the femur load cell location (or anywhere else in the Hybrid III KTH complex) are different from the forces at corresponding locations in the cadaver (Donnelly and Roberts 1986, Masson and Cavallero 2003, Rupp et al. 2005). This suggests that either the response biofidelity of the Hybrid III dummy needs to be improved so that it produces similar KTH forces as the human, or that the KTH injury criteria need to be adjusted before the current Hybrid III ATD can be used to assess KTH injury risk in frontal crashes.

Typically, this adjustment would be developed empirically, using data from studies in which the knees of cadavers and ATDs are loaded using similar loading conditions, such as those by Donnelly and Roberts (1986) and Rupp et al. (2005). However, the empirical approach to adjusting injury criteria is only valid if the experimental knee-loading conditions span those that occur in crashes, which those reported in previous studies do not. In particular, the force-deflection characteristics of the surfaces used to load the knees in previous studies were either linear elastic or hyperelastic, and therefore do not represent current real-world knee bolsters, many of which are likely exhibit a force-limiting behavior. As a result, the relationships between forces measured by ATD femur load cells and force in the cadaver KTH developed from existing experimental data would not apply to many of the knee-loading conditions that are likely to occur in real-world crashes.

Figure 1 illustrates how knee bolsters with different force-deflection characteristics can produce different relationships between force applied to the dummy and human knee under similar loading conditions. For the linear elastic (constant stiffness) and hyperelastic knee bolsters, force applied to the knee is higher for the Hybrid III than for the similar-sized cadaver because the Hybrid III KTH is stiffer and has more tightly coupled mass than the cadaver KTH complex and therefore penetrates further into the knee bolster. For a force-limiting knee bolster, the Hybrid III knees still penetrate further into the knee bolster than the cadaver, but the peak forces applied to both the Hybrid III and cadaver knees are the same if the knees of both the Hybrid III and cadaver penetrate into the force-limiting region.

As a consequence of the differences in force applied to the knees of the cadaver and Hybrid III by each type of knee bolster, the relationships between force measured by the Hybrid III femur load cell and the risk of KTH injury (which is a function of force produced at the cadaver knee and hip) will vary with the force-deflection characteristics of the surface loading the knee. Because of this, and because previous research demonstrates that the knee-impact response of the cadaver varies with loading rate and loading duration (Atkinson et al. 1997, Yoganandan et al. 2001, Rupp 2006), an unreasonably large number of cadaver and Hybrid III knee-impact tests would need to be conducted to empirically define the relationships between forces in the human KTH and Hybrid III femur force measurements.

GENERAL APPROACH

Because a purely experimental approach is not feasible, this study used a computational approach to define relationships between forces measured by Hybrid III femur load cells and the risk of human KTH injury. This approach involved (1) developing and validating a lumped-parameter model of the Hybrid III midsize male ATD and then (2) performing simulations in which this model and the lumped parameter midsize male cadaver model (Rupp et al. 2008) were loaded by knee bolsters with a wide range of force-deflection characteristics. Results of these simulations were used to establish relationships between the risk of injury to the human cadaver KTH complex and forces measured by Hybrid III midsize male femur load cells. These relationships were then scaled using established techniques to develop new injury criteria for the Hybrid III small-female ATD.

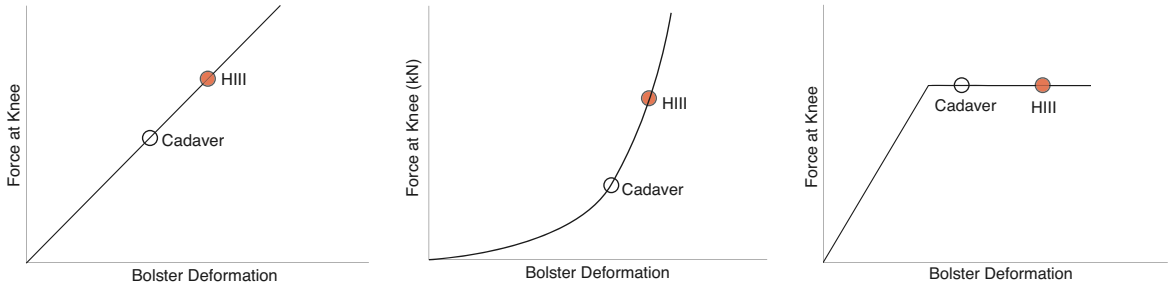

Figure 1. Force-deflection characteristics from linear-elastic (left), hyperelastic (middle), and force-limiting knee bolsters (right) illustrating peak applied force levels at the knee for midsize-male cadavers and the midsize-male Hybrid III.

DEVELOPMENT OF A HYBRID III LUMPED PARAMETER MODEL

The one-dimensional lumped parameter model that was developed to simulate the response of the Hybrid III midsize male ATD to symmetric knee loading is shown in Figure 2. This model represents the response of one side of the Hybrid III and is identical in form to the lumped parameter model that Rupp et al. (2008) used to describe the human cadaver knee impact response and to predict the drop in force between the knee and the hip. The methods used to develop the model involved defining known parameters from physical measurements of ATD components and identifying unknown parameters by simulating physical tests in which the knees of the a Hybrid III ATD were loaded and varying unknown model parameters were varied until predicted responses matched experimental results.

Model Formulation

There are 21 parameters in the Hybrid III model, including 7 masses, 6 springs, 6 damping coefficients, and two forces. Most of these parameters are known or can be inferred from the results of a series of physical tests in which the knees of a seated Hybrid III midsize male ATD were symmetrically loaded using the 1.2 m/s, 3.5 m/s, and 4.9 m/s loading conditions described by Rupp et al. (2008).

Table 1 summarizes the values for masses in the Hybrid III model. The static masses of the dummy knee, femur load cell, femur, and hip casting combine to form mA. Similarly, mB is also made up of the static masses of the dummy pelvis and thigh flesh. The stiffness and damping coefficients describing the coupling between the knee, femur, pelvis, and pelvis flesh were set so that the masses of the knee/femur (mA), the mass of the pelvis (mB), and the mass of the pelvis flesh (mC) were tightly coupled. Support for this is provided by the similarity in the magnitude and the phasing of femur and pelvis acceleration histories measured in symmetric knee impact tests performed on the Hybrid III ATD (Rupp et al. 2005). Because pelvis flesh is tightly coupled to the pelvis, it was not necessary to describe the mass of the pelvis flesh independently of that of the pelvic bone. Therefore, mB was set to the one half of the entire mass of the Hybrid III pelvis plus pelvis flesh and mC was set to a low value (0.001 kg).

Coupling between masses was described using linear springs and dampers in parallel, as shown in Figure 2, because this arrangement is thought to represent the simplest combination of elements that can appropriately describe the coupling of body segments across a wide range of knee impact conditions. Further, this arrangement was able to describe the response of the human cadaver to knee impact loading over a wide range of loading conditions and was therefore thought to be capable of modeling ATD response.

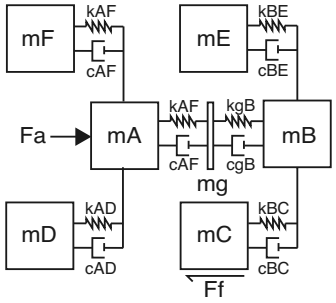

Figure 2. Lumped-parameter model.

Table 1. Descriptions of Masses in Hybrid III Midsize Male Lumped-Parameter Model

Mass	Descriptions
mA	Mass of knee, knee flesh, femur load cell, femur, and hip casting
mB	Mass of pelvis and flesh that is coupled to the pelvis
mC	Mass of the pelvis flesh
mD	Mass of leg below knee that is effectively coupled to the KTH
mE	Mass of torso that is effectively coupled to the pelvis
mF	Mass of thigh flesh that is coupled to femur
mg	Mass between femur and pelvis (set to 0.001 kg for all tests, needed so that femur force-deflection characteristics could be specified separately from those of the hip joint)

ATD Tests Used for Model Development

The ATD tests that were simulated to establish unknown parameters in the model are reported in the NHTSA biomechanics database (Test series ID NBED0607, Test Numbers 9346-9385). The methods for these tests are described by Rupp et al. (2005) and Rupp et al. (2008) and are therefore only summarized here.

The apparatus used in the Hybrid III tests is illustrated in Figures 2a and 2b. The apparatus functions by pneumatically accelerating a weighted platform into the knees of a stationary test subject. The velocity of the platform was set to be 1.2 m/s, 3.5 m/s, or 4.9 m/s just prior to impact. These velocities were used along with padding on the knee impact surfaces to produce knee loading rates and peak femur forces that were close to the 5th, 50th, and 95th percentiles of peak femur forces and loading

rates produced in FMVSS 208 and NCAP tests conducted between 1998 and 2004 (Rupp et al. 2008). For all tests, the ATD was seated in an upright posture with the knees at a 90˚ angle. The feet were supported by a platform whose height was adjusted to maintain this angle. The pelvis was supported by a force plate that measured the friction force produced by the pelvis flesh interacting with the platform. The ATD's feet were also supported by a different platform, the height of which was set so that the centerline of the impactor was aligned with the most forward surface on the knee. The Hybrid III midsize male ATD used in these tests was instrumented with a 6-axis femur load cell and triaxial accelerometer blocks were attached to the shaft of the femur, the pelvis, and the spine box. Prior to all tests, the knee response was verified by repeating the knee calibration test (SAE Dummy Testing and Equipment Subcommittee, 1998).

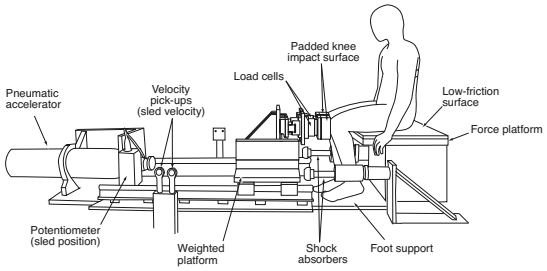

Figure 2a. Side-view (top) illustration of apparatus used to characterize ATD response.

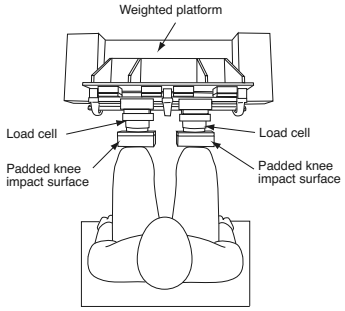

Figure 2b. Top-view (bottom) illustration of apparatus used to characterize ATD response.

Establishing Values for Unknown Model Parameters

Of the 21 model parameters (7 masses, 6 springs, 6 damping coefficients, and 2 forces), 15 are known and 6 are unknown, although reasonable bounds on all unknown parameters can be established. Table 2 lists values and data sources for the known parameters and bounds on the unknown parameters, which include the amounts of leg and torso mass that can couple to the KTH complex and the spring stiffnesses and damping coefficients that describe this coupling. Rows containing these unknown parameters are highlighted in Table 2.

Table 2. Parameters and Bounds on Parameter Values Used in Hybrid III Model

Element	Source	Value/Constraints
Fa	Test data	NA (from test data)
Ff	0.5*(Friction force applied to pelvis flesh)	NA (from test data)
mA	Static mass of Hybrid III knee + femur load cell + femur + hip casting mass	6.68 kg
mB	0.5*(Static mass of Hybrid III pelvis)	7.11 kg
mC	mC is rigidly coupled to mB and the mass of the pelvis flesh is treated as part of the pelvis.	0.001 kg
mD	Determined from optimization	0.1 < mD < 4.5 kg
mE	0.5*(Static mass of Hybrid III torso).	0.1 < mE < 20.8 kg
mF	Static mass of Hybrid III thigh flesh.	0.9 kg
mg	Set to near zero so that it has no effect on simulation results.	0.001 kg
k_{Ag}, c_{Ag}	Set to high values so that knee/femur/hip casting are effectively rigid.	k_{Ag} = 1,000 kN/m c_{Ag} = 25,000 Ns/m
k_{gB}, c_{gB}	Set to high values the coupling between the femur and pelvis is effectively rigid.	k_{gB} = 1,000 kN/m c_{gB} = 25,000 Ns/m
k_{BC}, c_{BC}	Set to high values the coupling between the femur and pelvis is effectively rigid.	k_{BC} = 1,000 kN/m c_{BC} = 25,000 Ns/m
k_{AD}, c_{AD}	Determined from optimization.	100 < k_{AD}< 50000 N/m 10 < c_{AD}< 5000 Ns/m
k_{BE}, c_{BE}	Determined from optimization.	0.01 < k_{BE} < 20 kN/m 10 < c_{BE} < 5000 Ns/m
k_{AF}, c_{AF}	Set to high values the coupling between the leg and knee is effectively rigid.	k_{BC} = 1,000 kN/m c_{BC} = 25,000 Ns/m

Bounds on the leg and torso masses were set so that the masses were varied between 0.1 kg and their static mass. Bounds on the coefficients describing the coupling of the masses to the KTH were set so that the coupling varied from loose (little effect on forces and accelerations predicted by the model) to stiff (effectively rigidly coupled).

The masses of the leg and torso that are effectively coupled to the KTH complex and the parameters describing the coupling between these masses and the KTH complex were determined using optimization techniques that are similar to those to define unknown parameters in the cadaver model by Rupp et al. (2008). In brief, the knee impact force histories from the 4.9 m/s test described above were applied to the knee of the Hybrid III model (mA). Unknown model parameters were then varied using a simulated annealing algorithm in Mathematica 6.0 (Wolfram Inc., Chicago, IL) until the until the sum of the areas between predicted and experimentally measured femur force and acceleration histories, and pelvis-acceleration histories in the direction of impact loading (x axis for pelvis and z-axis for femur) were minimized. For all model development simulations, half of the friction force measured by the force platform on which the ATD was seated was applied to the pelvis flesh (mC). Predicted femur force was calculated by inertially adjusting the predicted force at the connection between mA and mg using femur acceleration and the mass between mg and the femur load cell location (3.9 kg).

Table 3 shows the model parameters that produced the best fit of the experimental femur force, femur acceleration, and pelvis acceleration histories from the 4.9 m/s impact velocity. Figure 3 compares the femur force history predicted by the Hybrid III model to femur forces measured in repeated symmetric knee impacts performed using the Hybrid III midsize male ATD using the 4.9 m/s loading condition. Figures 4 and 5 make similar comparisons for femur and pelvis accelerations, respectively. All model predictions are within the range of experimentally measured responses from repeated tests on the same ATD.

Table 3. Parameters Used in Hybrid III Model

Param	Description	Final Value
mA	Static mass of Hybrid III knee, femur lc, femur, and hip casting	6.68 kg
mB	0.5*(Static mass of Hybrid III pelvis)	7.11 kg
mC	Mass of pelvis flesh (assumed to be tightly coupled to the pelvis)	0.001 kg
mD	Mass of leg from optimization	0.5 kg
mE	Coupled torso mass of, from optimization	5.4 kg
mF	Static mass of Hybrid III thigh flesh	0.9 kg
mg	Set to near zero so that it has no effect on simulation results	0.001 kg
k_{Ag}, c_{Ag}	Stiffness and damping coefficient between knee/femur and hip	k_{Ag} = 3,000 kN/m c_{Ag} = 25 kNs/m
k_{gB}, c_{gB}	Stiffness and damping coefficient of hip	k_{gB} = 3,000 kN/m c_{gB} = 30 kNs/m
k_{BC}, c_{BC}	Stiffness and damping coefficient between pelvis and pelvis flesh	k_{BC} = 1,000 kN/m c_{BC} = 25 kNs/m
k_{AD}, c_{AD}	Stiffness and damping coefficient between leg and knee/femur	k_{AD}= 13.52 kN/m c_{AD}= 1 kNs/m
k_{BE}, c_{BE}	Stiffness and damping coefficient between pelvis and torso	k_{BE}= 0.5 kN/m c_{BE}= 1.5 kNs/m
k_{AF}, C_{AF}	Stiffness and damping coefficient between thigh flesh and femur	k_{BC} = 100 kN/m c_{BC} = 25 kNs/m

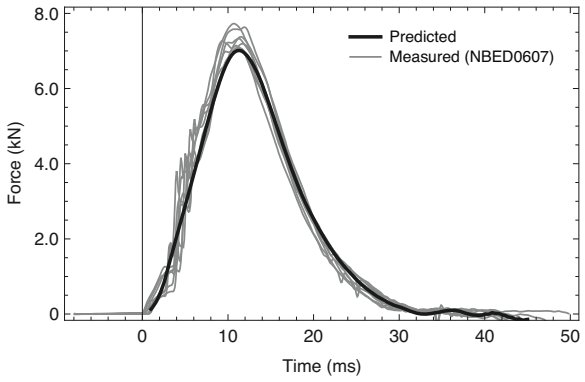

Figure 3. Predicted and experimentally measured femur force from 4.9 m/s tests.

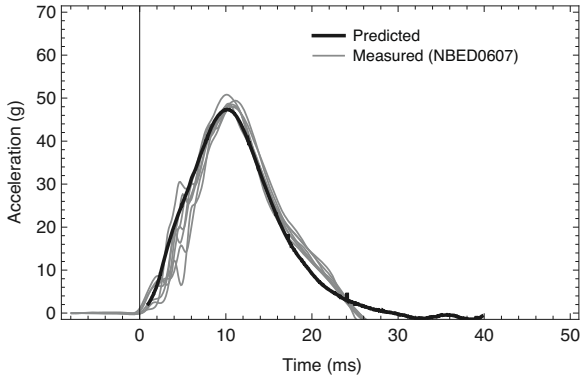

Figure 4 Predicted and experimentally measured femur Z-axis accelerations from 4.9 m/s tests.

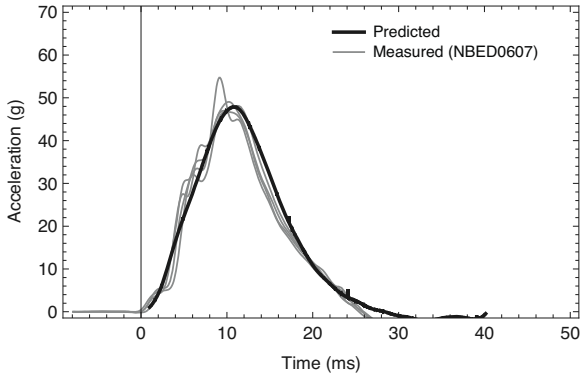

Figure 5. Predicted and experimentally measured pelvis X-axis accelerations from 4.9 m/s tests.

Model Validation

Model validation was performed by applying the average force histories applied to the Hybrid III ATD knees in repeated tests at the 3.5 m/s and 1.2 m/s impact velocities to the knee of the Hybrid III model and then comparing experimentally measured and predicted femur force, femur acceleration, and pelvis acceleration histories. To further verify that the parameters describing masses and the coupling of masses were appropriate, knee impacts in which the torso and thigh flesh had been removed from a Hybrid III midsize male ATD were also simulated. These tests were conducted using the 1.2 m/s, 3.5 m/s, and 4.9 m/s impact conditions described above. Predicted and measured femur force and acceleration, and pelvis acceleration, were compared. To simulate tests in which the dummy torso and the dummy thigh flesh were removed, the masses of these components in the lumped parameter model were set to 0.001 kg, so as to be close to zero but still high enough so that model predictions were stable.

Model validation results are shown in Figures 6 through 11. Figures 6 through 8 show that model predictions for femur force, femur z-axis acceleration, and pelvis x-axis acceleration from whole ATD tests at 3.5 m/s, respectively, are within the range of experimental results. Although not shown in this paper, a similar finding held for simulations of whole-dummy tests at 1.2 m/s.

Figures 8 through 11 demonstrate that model predictions of femur force, femur acceleration, and pelvis acceleration are within the ranges of experimentally measured values for simulations of tests in which thigh flesh and torso were removed at the 3.5 m/s impact condition. Simulations of the tests in which only the torso was removed (not shown here) indicate similar agreement with experimental results.

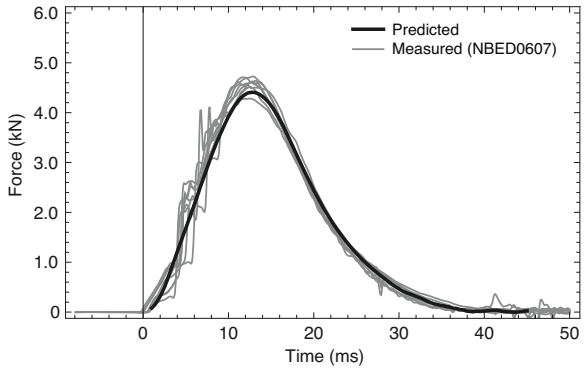

Figure 6. Predicted and experimentally measured femur forces from tests at 3.5 m/s with the whole Hybrid III midsize male ATD.

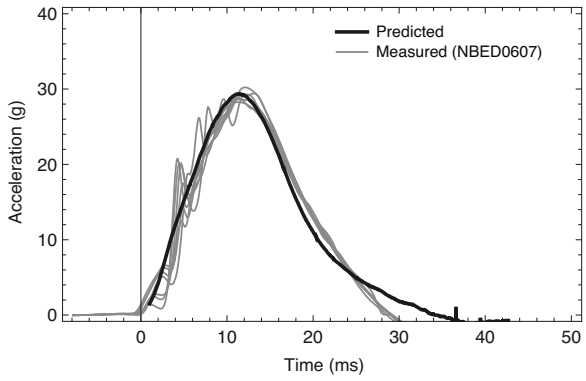

Figure 7. Predicted and experimentally measured femur z-axis accelerations from tests at 3.5 m/s with the whole Hybrid III midsize male ATD.

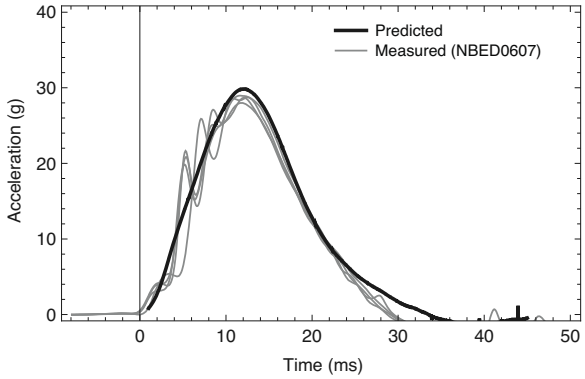

Figure 8. Predicted and experimentally measured pelvis x-axis accelerations from tests at 3.5 m/s with the whole Hybrid III midsize male ATD.

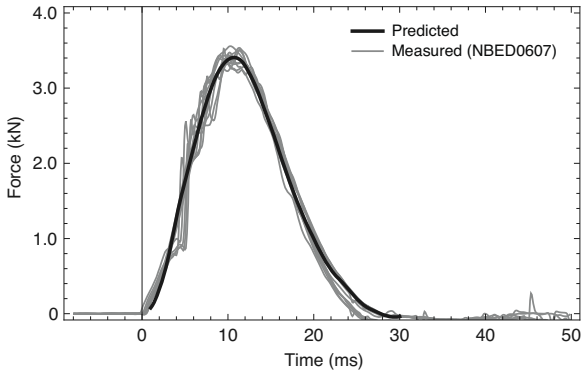

Figure 9. Predicted and experimentally measured femur forces from 3.5 m/s tests with the dummy torso and thigh flesh removed.

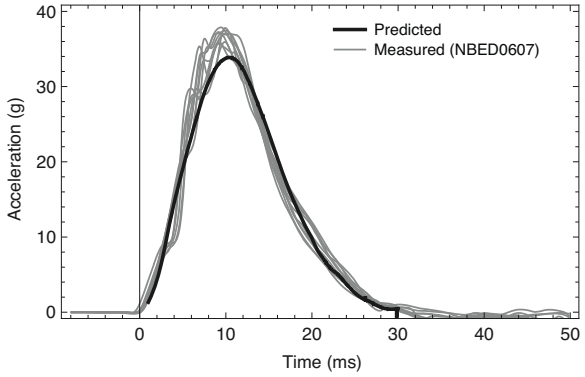

Figure 10. Predicted and experimentally measured femur z-axis accelerations from 3.5 m/s with the dummy torso and thigh flesh removed.

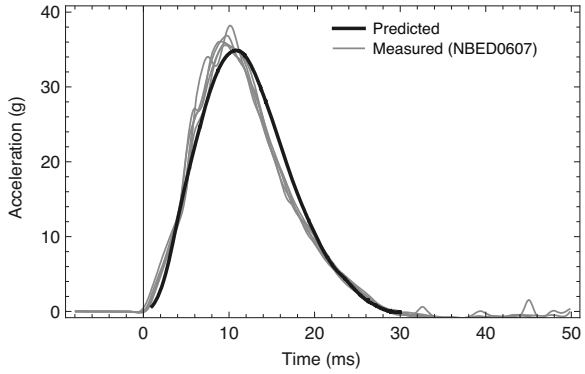

Figure 11. Predicted and experimentally measured pelvis x-axis accelerations from 3.5 m/s tests with the dummy torso and thigh flesh removed.

SIMULATIONS TO ESTABLISH INJURY ASSESSMENT CRITERIA

Simulations to Explore Relationships Between Peak Force at the Femur Load Cell and Peak Force at the Cadaver Hip

The relationship between Hybrid III peak femur force and risk of knee/distal femur injury is specified by existing injury criteria (i.e., the knee/distal femur risk curves reported by Kuppa et al. 2001 and Rupp et al. 2009). However, the relationship between peak force at the Hybrid III femur load cell and peak force at the human hip under similar knee-loading conditions is not known. Therefore, as a first step in developing new IARVs for the KTH complex, a series of simulations was performed to explore the relationships between peak forces in the cadaver and Hybrid III midsize male KTH complexes produced by similar knee-loading conditions.

In this series of simulations, the cadaver and Hybrid III models were loaded by simulated knee bolsters with three different types of force-deflection characteristics, including linear force-deflection (constant stiffness), bilinear force-deflection, and force-limiting. Figure 12 illustrates these force-deflection characteristics and shows how they were parameterized.

These three types of knee bolsters were selected because they span the range of force-deflection characteristics expected to occur in current production knee bolsters. In particular, a force-limiting knee bolster represents an ideal knee bolster design for a particular size of occupant because it limits the force applied to the knee while maximizing the amount of energy absorbed over the least amount of knee bolster compression. In contrast, for a

constant-stiffness knee bolster, the force applied to the knees increases linearly with compression of the bolster until the knees are completely stopped. A knee bolster with a bilinear force-deflection characteristic represents the scenarios where the stiffness of the knee bolster either suddenly decreases from yielding of components or suddenly increases because the occupant's knees bottom out the bolster.

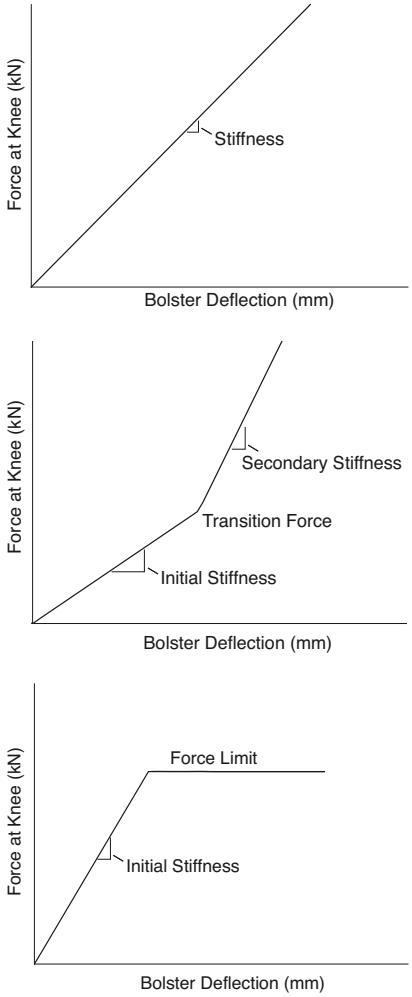

Figure 12. Illustrations of knee bolster force-deflection characteristics used in simulations: constant stiffness (top), bilinear force-deflection (middle), and force-limiting (bottom).

Table 4 lists the ranges of knee bolster force-deflection characteristics and impact velocities used in the simulations. These ranges were selected so that the simulated knee-loading conditions produced peak Hybrid III femur forces and loading rates that span the upper portion of the ranges of those that occur in FMVSS 208 and US NCAP tests. Knee bolster stiffness in these simulations was varied from 50 N/mm to 450 N/mm. The lower bound on knee bolster stiffness is based on data reported by Rupp et al. (2007), who loaded isolated production knee bolsters with cadaver knees. The upper bound on knee bolster stiffness is based on simulation results reported by Rupp et al. (2008), which indicated that a bolster stiffness above 450 N/mm produces knee-loading rates in excess of 2 kN/ms, which previous studies have associated with knee loading by a rigid (non-knee-bolster like) surface (Rupp et al. 2002, Rupp et al. 2007).

Table 4. Ranges of Parameters Used in Simulations

Bolster Type	Parameter Ranges
Force Limiting	Initial Stiffness: 200 to 450 N/mm Force Limit: 4 kN to 18 kN, Velocity: 3 to 8 m/s
Linear Force-Deflection	Stiffness: 50 to 450 N/mm Impact velocity: 2 to 8 m/s
Bilinear Force-Deflection	Initial stiffness: 50 to 450 N/mm Transition force: 2 to 8 kN Secondary stiffness: 50 to 250 N/mm Impact velocity: 2 to 8 m/s

To simulate knee-to-knee bolster loading, the lumped-parameter model was modified so that the force-based driving function was replaced by a 500-kg impactor mass, mI, which was connected to the knee by a spring. The stiffness of this spring, kIA, represents the combined stiffness of the impactor and the knee surface. The modified model is shown in Figure 13.

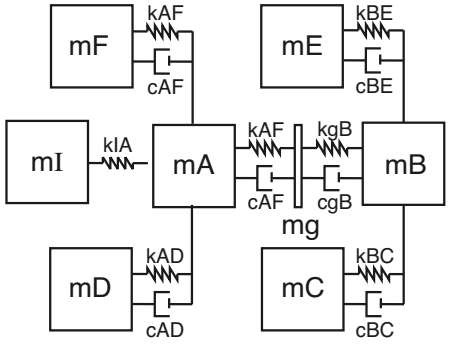

Figure 13. Lumped-parameter model with knee-bolster mass (mI).

Figure 14 compares the range (shaded area) of peak femur forces and loading rates produced in the simulations with the Hybrid III lumped-parameter model using the combinations of loading conditions listed in Table 4, to peak femur forces and loading rates from FMVSS 208 and NCAP tests from 1998-2004. To generate the data points in Figure 14, loading rate was calculated by taking the slope of the force history from the Hybrid III femur load cell

between 15% and 85% of peak force. Figure 14 shows that the knee-loading conditions used in the simulations span the upper portion of loading rates that occur in staged frontal crashes. As a result, these simulations represent knee-impact forces that are likely to produce significant risks of KTH fractures and are therefore relevant to exploring the relationship between Hybrid III femur force and force at the cadaver hip as it pertains to KTH injury assessment

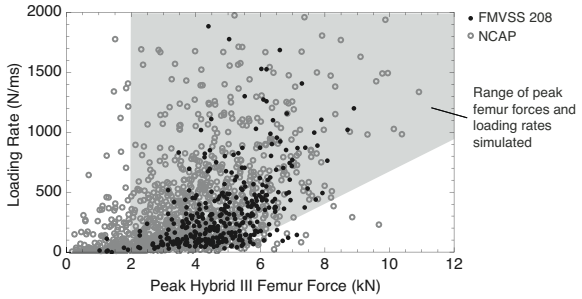

Figure 14. Comparison of peak Hybrid III femur forces and loading rates from FMVSS 208 and NCAP tests to combinations of similar parameters produced in all simulations.

Figures 15 and 16 illustrate the relationships between forces at different locations in the Hybrid III and cadaver KTH complexes that were produced by simulations with the Hybrid III and cadaver lumped-parameter models. Figure 15 shows forces at the knee, femur load-cell of the Hybrid III ATD, and hip that have been normalized by dividing the peak applied force at the knee. As illustrated by Figure15, the percentage of peak force at the Hybrid III knee that is transmitted to the femur load cell and the percentage of peak force applied to the cadaver knee that is transmitted to the hip are approximately 77% and 55%, respectively. Importantly, these values are relatively constant over the range of simulated knee-loading conditions. This finding indicates that knee loading by a surface that applies the same force to the knees of the cadaver and the Hybrid III (i.e., a force-limiting knee bolster) will produce a ratio of peak force at the femur load cell to peak force at the cadaver hip of 1.4 (0.77/0.55).

Because a singular relationship exists between peak force at the Hybrid III femur load cell and peak force at the cadaver hip for knee loading by a force-limiting knee bolster when both the cadaver and the Hybrid III load the bolster to the force limit, peak femur force can be used to predict the risks of both knee/distal femur injury and hip injury. For example, as illustrated by the thick black and gray lines in Figure 16, knee loading by a force-limiting knee bolster that applies a force of 8.3 kN to both the Hybrid III and cadaver knees will produce a peak Hybrid III femur force of ~6.4 kN and force at the cadaver hip of ~4.6 kN (6.4/1.4). Using the knee/distal femur and hip injury risk curves reported in Equations 1 and 2 in the following section of this paper, 6.4 kN at the Hybrid III femur load cell corresponds to an ~8% risk of knee/distal femur fracture and a ~25% risk of hip fracture/dislocation.

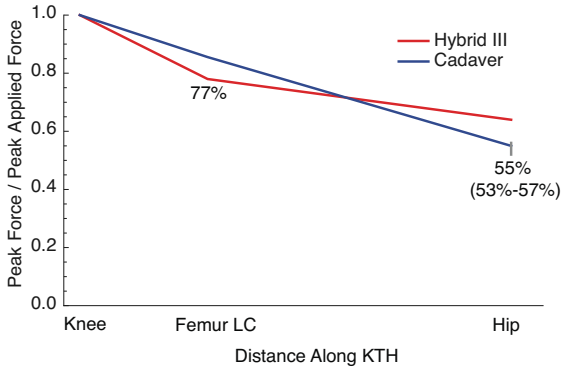

Figure 15. Percentages of force transmitted from the knee to the cadaver hip and from the knee to the Hybrid III femur load cell produce in all simulations.

For knee loading by knee bolsters that are not-force limiting (or loading by a force-limiting knee bolster that is not impacted at a velocity sufficient to generate a force in excess of its force limit), the peak force applied to the Hybrid III knee will always be greater than the peak force applied to the cadaver knee. This is because the Hybrid III has greater effective mass and stiffness than the cadaver and will therefore penetrate further into the knee bolster, regardless of bolster force-deflection characteristics.

Figure 16 illustrates the implications of the differences in knee impact force produced by different types of knee bolsters on the relationships between peak forces at in the Hybrid III and cadaver KTH complexes for all loading conditions that produce a 25% risk of hip fracture. Since all forces in Figure 16 are associated with the same risk of injury to the cadaver hip, they are associated with the same force at the cadaver hip (4.56 kN). As discussed earlier, the thick gray and black lines in Figure 16 represent the Hybrid III and cadaver responses produced by knee loading by a force-limiting knee bolster. The gray shaded area in Figure 16 illustrates how, for knee loading by a knee bolster that is not force-limiting (e.g., a constant-stiffness bolster) a higher peak force will be applied to the

Hybrid III knee and that this produces greater differences between peak Hybrid III femur force and force at the cadaver hip. As a result, knee loading by a force-limiting knee bolster will always produce the smallest possible difference between peak force at the Hybrid III femur load cell and peak force at the cadaver hip.

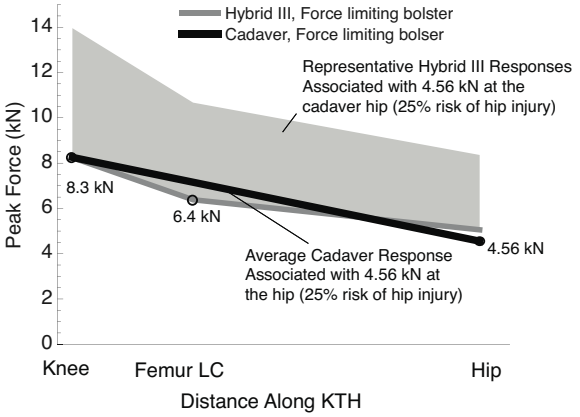

Figure 16. Relationships between peak forces at different locations in the cadaver and Hybrid III KTH complexes associated with a 25% risk of KTH injury (i.e., a force of 4.56 kN at the cadaver hip).

In summary, Figure 16 illustrates that there is no singular relationship between peak force at the Hybrid III femur load cell and peak force at the cadaver hip that is valid over the full range of knee bolster force-deflection characteristics that are thought to occur in production vehicles. As a result, it is not reasonable to base IARVs for the entire KTH complex on peak Hybrid III force alone. However, as discussed below, it is possible to develop injury assessment criteria for the hip that define the set of femur force histories that can be associated with a risk hip injury in excess of a target value.

Development of KTH Injury Assessment Criteria for the Hybrid III Midsize Male ATD

Simulations with the cadaver model reported by Rupp et al. (2008) demonstrate that the risk of hip injury is higher than the risk of knee or distal femur injury over most of the range of loading conditions that occur in frontal crashes. However, these simulations also demonstrate that the likelihood of knee/distal femur injury is higher than the likelihood of hip injury for high-rate, short-duration knee loading. This is because under these conditions, the femur has not displaced enough to recruit sufficient pelvis mass to produce a force at the hip that corresponds to a risk of hip injury that is greater than the risk of knee/distal femur injury associated with the force applied to the knee.

These observations suggest that injury criteria for the entire KTH should assess the risk of knee/distal femur injury for high-rate and short-duration loading, and should assess the risk of hip injury for the lower-rate, longer-duration loading conditions that are more typical of those produced in frontal crashes. Since a comprehensive KTH injury assessment criterion must determine whether to assess hip or knee/distal femur injury risk, such a criterion will need to incorporate a parameter that relates to femur displacement that can be measured by the Hybrid III femur load cell. For the injury assessment criteria development effort described below, this parameter was impulse (the integral of the femur force history between two points in time).

When plotted, the combination of the Hybrid III femur forces associated with a specified level (e.g., 25%) of knee/distal femur injury risk and hip injury risk along with the transition impulse that defines the transition between the two methods of injury assessment takes the form illustrated in Figure 17. Since the generalized injury assessment criterion shown in Figure 17 is a boundary and not a single value, or set of values, it has been termed an "injury assessment reference boundary." The three parts of the injury assessment reference boundary are called the lower- force limit (or hip-injury risk-based limit), the transition impulse, and the upper-force limit (or knee/distal-femur risk-based limit).

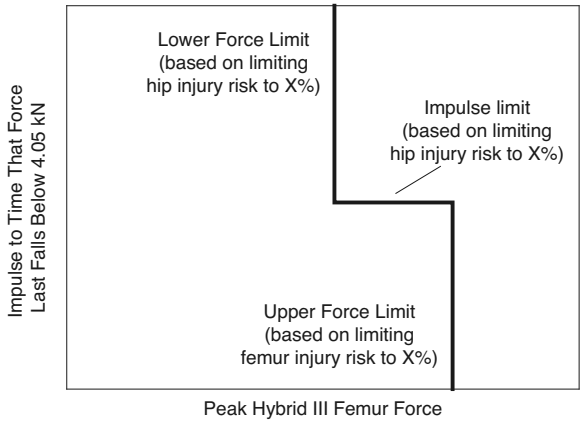

Figure 17. Generalized form of the KTH injury assessment reference boundary.

For all injury assessment reference boundaries, the transition impulse was determined by integrating Hybrid III femur force from the start of loading to the time that force last fell below 4.05 kN, as illustrated

in Figure 19. This value was chosen because it is the Hybrid III femur force that corresponds to the lowest hip fracture force of 2.89 kN reported by Rupp et al. (2003) – i.e., 4.05 = 1.4 times 2.78.

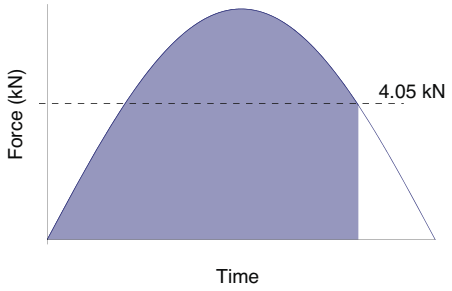

Figure 18. Impulse calculation.

Upper-force limit – The forces associated with the upper-force limit for a given level of knee/distal femur injury risk and hip injury risk were established using the injury risk curve in Equation 1.

$$Risk_{Knee/DistalFemurFX} = 1 - Exp\left[Exp\left[\frac{\ln[F] - 2.514}{0.2611}\right]\right] \quad [1]$$

where F is the peak compressive force measured by the Hybrid III femur load cell in kN and risk lies between zero and one.

Equation 1 is a slightly modified version of the risk curve that underlies the current FMVSS 208 maximum femur force criterion (Kuppa et al. 2001) that accounts for censoring in the knee impact fracture force data that were used to develop the current FMVSS 208 KTH injury risk curve (Rupp et al. 2009). This risk curve defines the risk of knee/distal femur injury in terms of peak force at the Hybrid III femur load cell.

Lower-force limit – Equation 2 defines the relationship between hip injury risk and force at the human hip as a function of occupant stature and hip posture (Rupp et al. 2009):

$$Risk_{HipFX} = \Phi\left[\frac{\ln[F] - (0.2141 + 0.0114s)*(1-(f-a)/100)}{0.1991}\right] \quad [2]$$

where, Φ is the cumulative distribution function of the standard normal distribution,
F is peak force transmitted to the hip in kN,
s is the stature of the target population for the risk curve (178 cm for midsize males),
f is the hip flexion angle in degrees, and
a is the hip abduction angle in degrees.

For developing midsize male injury assessment criteria, a stature of 178 cm was used and hip posture was set to 15° hip abduction and 30° flexion, which has been estimated to represent the typical hip posture at the time of peak femur force in full frontal crashes (Rupp et al. 2008). For reference, Figure 19 compares hip and femur injury risk curves.

Once the force at the human hip associated with a given level of hip injury risk was calculated, the lower-force limit was determined by multiplying this value by 1.4. As discussed above, this value represents the ratio of peak femur force at the Hybrid III femur load cell to peak force at the cadaver hip for knee loading by a force-limiting knee bolster, which, by virtue of applying the same force to the Hybrid III ATD and cadaver knees, produces the smallest possible difference between peak Hybrid III femur force and force at the cadaver hip.

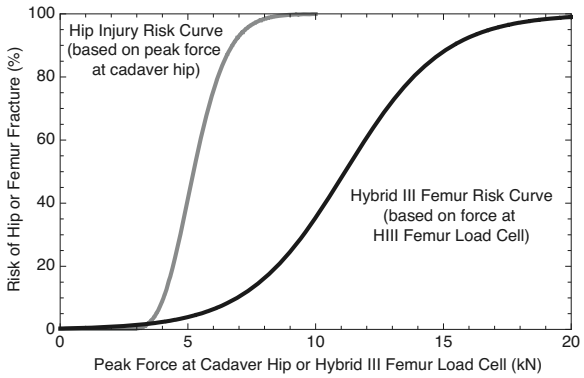

Figure 19. Femur injury risk curve and hip injury risk curve developed using with a stature of 178 cm and 15° abducted and 30° flexed hip posture.

Transition impulse–For a given level of KTH injury risk, the transition impulse was established by performing simulations with the Hybrid III and cadaver models to identify the smallest value of impulse that can be associated with a risk of hip injury above a specified percentage for peak femur forces between the upper and lower-force limits. Because the goal of these simulations was to establish the minimum impulse value associated with a given risk of hip injury, all of the transition impulse development simulations were performed using the highest knee bolster stiffness that was reasonable, which, for reasons previously noted, was 450 N/mm. The rationale for this approach was that the highest possible knee-loading rate produces the shortest duration of applied force, and therefore the smallest impulse, necessary to generate a specific force at the hip (and a specific level of hip injury risk).

When the knees of the cadaver model were loaded using a knee bolster with a stiffness of 450 N/mm, there was only a single knee impact velocity that produced a force at the cadaver hip associated with the target level of hip injury risk. However, this combination of impact velocity and bolster stiffness always produced a peak Hybrid III femur force that was greater than the value associated with the upper-force limit. Since the transition impulse does not apply to this loading condition, the force-deflection characteristics of the knee bolster were modified so that the knee bolster was force-limiting and had a force limit that produced a peak femur force that corresponded to the level of risk associated with the transition impulse. The impulse of the femur force produced by this knee bolster stiffness and impact velocity, calculated in the manner described above, represents the minimum impulse that can be associated with a given level of hip injury risk. This finding was confirmed by an alternate approach to transition impulse development in which knee bolster force-deflection characteristics and impact velocity were varied until the minimum impulse necessary to produce a given risk of hip injury was determined for forces between the upper and lower-force limits.

Example Development of 25% Risk Boundary–A more detailed example of how the injury assessment reference boundaries were developed is provided below and in Figure 20 for the injury assessment reference boundary corresponding to a 25% risk of KTH injury. Based on Equation 2, peak force at the cadaver hip associated with a 25% risk of hip injury is 4.56 kN. Multiplying this value by 1.4 indicates that the lower-force limit is 6.38 kN. As illustrated in the left column of Figure 20, the lower-force limit is produced through knee loading by a force limiting knee bolster with a force limit of 8.25 kN, which produces 4.56 kN at the cadaver hip and 6.38 kN at the Hybrid III femur load cell. As discussed above, this is because a force limiting knee bolster produces the smallest possible Hybrid III femur force that can be associated with a 25% risk of hip injury. To produce the responses shown in the left column of Figure 20, an impact velocity of 6.25 m/s was used. This velocity was selected because it is large enough so that the cadaver model knee sufficiently compresses the knee bolster to exceed its force limit.

The middle part of Figure 20 shows the loading condition and simulation results that define the transition impulse for the 25% risk boundary. For reasons discussed above, this loading condition was determined by loading the knees of the cadaver and Hybrid III models with a force limiting knee bolster with an initial stiffness of 450 N/mm. The force limit for this knee bolster was set to 11.56 kN, which produces a peak Hybrid III femur force of 8.93 kN, which Equation 1 associates with a 25% risk of knee/distal femur injury.

Simulations with the cadaver model using these loading characteristics indicated that an impact velocity of 5.2 m/s produced peak force at the hip of 4.56 kN (i.e., a 25% risk of hip injury). Since a 5.2 m/s impact velocity produces a force at the cadaver knee that is below the bolster force limit, the cadaver knee does not penetrate far enough into the knee bolster to reach the limiting force, as shown in the top and bottom cells in the middle column of Figure 20. However, as is also shown in Figure 20, at this impact velocity, force at the Hybrid III knee reaches the force limit. The impulse of the Hybrid III femur force, calculated using the procedure shown in Figure 18, associated with this loading condition is 137.1 Ns. This value is the smallest impulse capable of producing a force at the hip in excess of the value associated with 25% KTH injury risk, provided that knee bolster stiffness is not greater than 450 N/mm and that peak Hybrid III femur force is less than the upper-force limit for knee/distal femur injury.

The right side of Figure 20 shows the results of a simulation that was performed to check the transition impulse of the 25% injury risk boundary. This simulation used the same knee-bolster force-deflection characteristics as those used to establish the lower-force limit (8.25 kN force limit with a 450 N/mm initial stiffness), and a knee-impact velocity that resulted in an impulse of 137.1 Ns at the Hybrid III femur load cell. As shown in the bottom right part of Figure 20, at this impact velocity, there is not a sufficient amount of impact energy to cause the force at the knee to exceed the knee bolster force limit for a duration that is long enough for force at the hip to exceed the value associated with a 25% risk of hip injury.

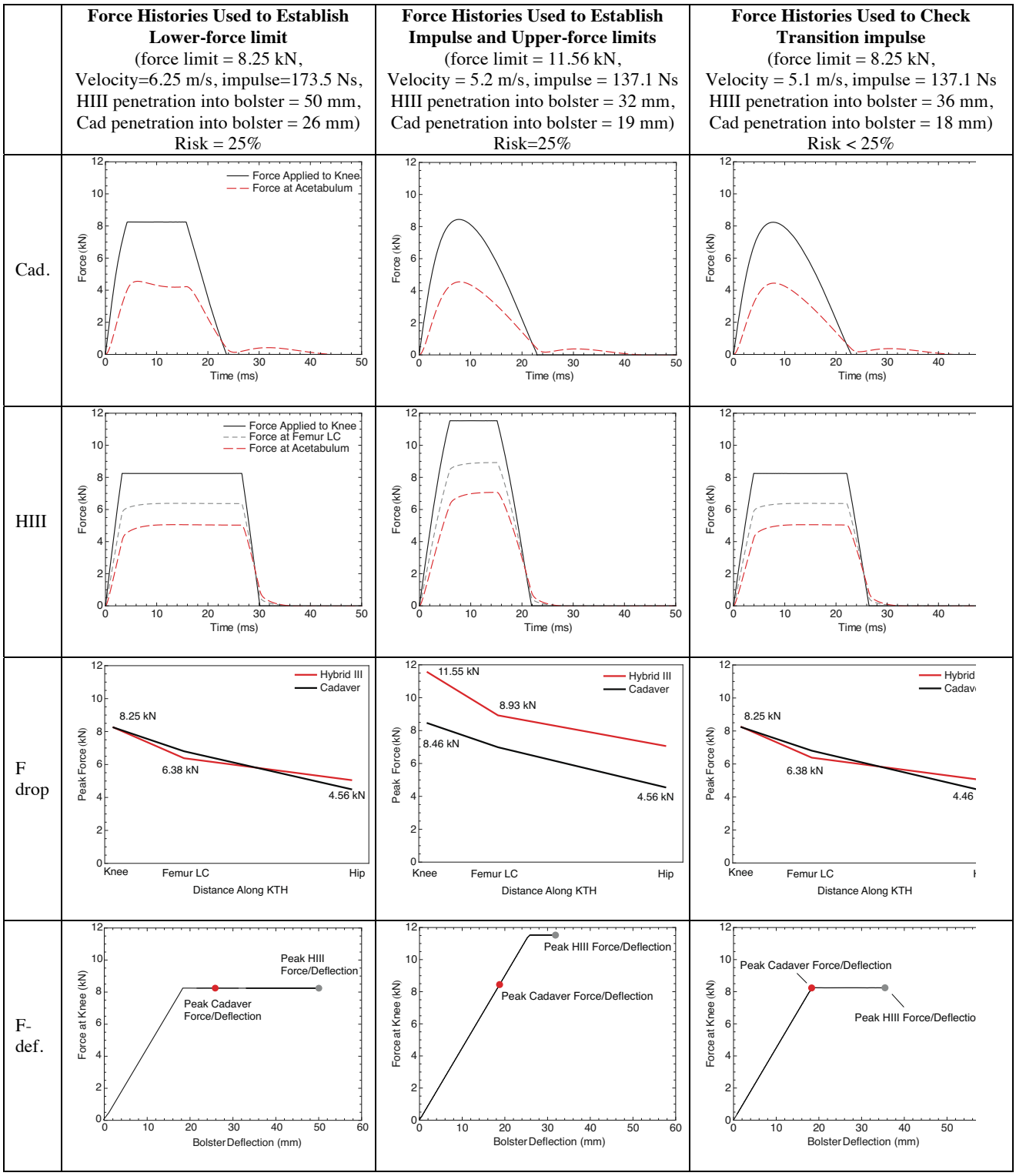

Figure 20. Force histories, plots of the decrease in force along the KTH, and knee bolster force penetration responses produced in simulations used to develop and check the upper and lower-force limits and the transition impulse associated with the 25% risk injury assessment reference boundaries.

Injury Assessment Risk Boundaries for Multiple Levels of KTH Injury Risk–Table 5 lists the lower-force limit, the transition impulse, and the upper-force limit associated with injury assessment reference boundaries for 3%, 5%, 10%, 15%, 20%, 25%, 30%, 35%, 40%, 45%, 50%, and 75% risk of KTH injury at a hip posture that is 30˚ flexed and 15˚ abducted (i.e., the typical posture at the time of peak femur force in an FMVSS 208 or NCAP test). The differences in the slopes of the femur and hip injury risk curves explain why the difference between the upper and, shown in Figure 17, the lower-force limits increases with the level of risk associated with each boundary. These same differences also explain why the upper and lower-force limits are equal at the 3% risk level. For reference, Figure 21 plots some of these injury assessment reference boundaries for each level of injury risk and Figure 22 plots each of the reference boundaries as a function of injury risk.

Table 5. Injury Assessment Reference Boundaries For 3% to 75% Risks of KTH Injury

Risk	Lower-force limit (kN) †	Transition impulse (Ns) †	Upper-force limit (kN)††
3	4.97	NA*	4.97
5	5.22	113.5	5.69
10	5.63	121.8	6.87
15	5.92	127.7	7.69
20	6.16	132.7	8.35
25	6.38	137.1	8.92
30	6.59	141.3	9.44
35	6.79	145.5	9.92
40	6.98	149.4	10.37
45	7.18	153.3	10.80
50	7.35	157.2	11.23
75	8.40	180.7	13.45

*Not applicable because the upper and lower-force limits are equal.

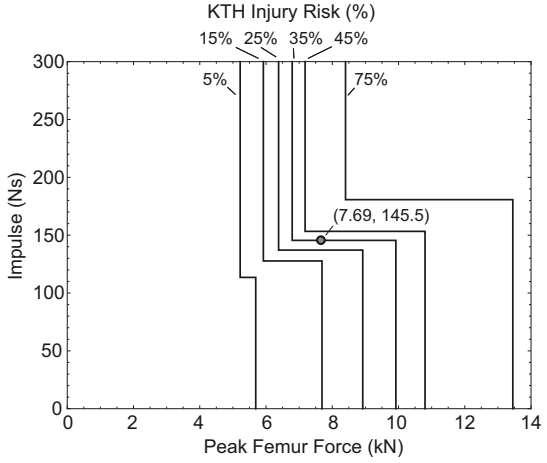

Figure 21. Select injury assessment reference boundaries.

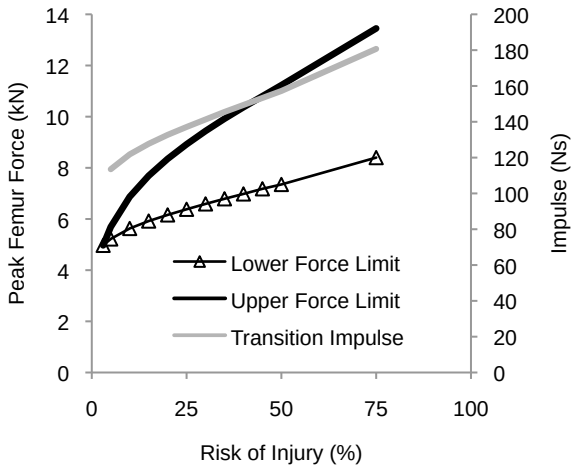

Figure 22. Lower force limit, upper force limit and transition impulse as functions of the associated level of injury risk.

Using the Injury Assessment Reference Boundaries to Estimate Hip and Knee/Distal Femur Injury Risk

The previous section described the development of injury assessment reference boundaries associated with specific levels of KTH injury risk. While each of these boundaries defines a pass/fail injury assessment criterion, like the current 10-kN maximum femur force criterion, no single boundary provides sufficient information to estimate the risks knee/distal femur and hip injury associated with a specified femur force history. However, when combined, multiple injury assessment risk boundaries can be used to estimate the risk of knee/distal femur injury and the maximum possible risk of hip injury associated with a Hybrid III femur force history. For example, based on the upper-force limit, a Hybrid III femur force history that is has a peak of 7.69 kN and an impulse of 145.5 Ns is associated with a 15% risk of knee/distal femur fracture based on Equation 1. The risk of hip fracture for this combination is the smaller of the risks of hip injury determined by comparing peak femur force to the lower force limit and impulse to the transition impulse. This approach is identical to determining which boundary passes through a particular combination of peak force and impulse. For example, as illustrated in Figure 21, a peak force of 7.69 kN and an impulse of 145.5 Ns are on the 35% risk boundary and are therefore associated with no more than a 35% risk of hip injury.

Checks on the Injury Assessment Reference Boundaries–As a check on the injury assessment reference boundaries listed in Table 5, peak Hybrid III femur force, impulse at the Hybrid III femur load

cell, and KTH injury risk were calculated from the set of Hybrid III and cadaver model predictions produced when the loading conditions in Table 4 were simulated. Combinations of peak femur force and impulse associated with KTH injury risks greater than the level of risk associated with each injury assessment boundary were then compared. For these comparisons, KTH injury risk was the maximum of the risk of injury to the hip predicted by the cadaver model and risk of injury to the knee/distal femur predicted by the Hybrid III model. Figure 23 shows that the 25% risk boundary defines all combinations of peak femur force and impulse that were associated risks of KTH injury greater than 25%. A similar finding held for all of injury assessment reference boundaries listed in Table 5.

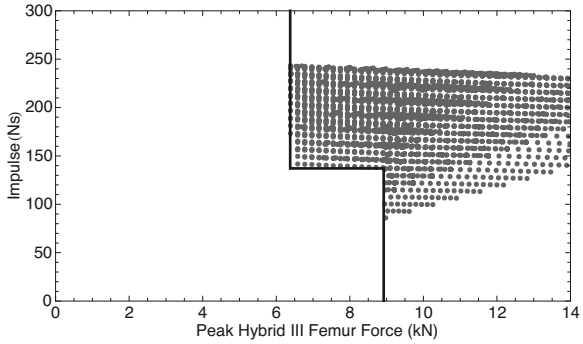

Figure 23. Comparison of 25% injury assessment reference boundary to combinations of peak femur force and impulse that produced risks of KTH injury greater than 25%.

Development of Injury Assessment Reference Boundaries for the Hybrid III Small-female ATD

The injury assessment reference boundaries listed in Table 5 only apply to the midsize male ATD. Development of injury assessment reference boundaries for the small-female ATD in the same manner that was used to develop the midsize male IARVs is currently not feasible, since it would require knee impact response data for similar-size female cadavers, which are not available. Consequently, injury assessment reference boundaries for the small-female ATD were developed using scaling techniques.

Mertz et al. (2003) used a factor of 0.679 to scale femur force in the Hybrid III midsize male to femur force in the Hybrid III small female based anthropometric and dimensional analysis considerations, so this factor was applied to scale the upper-force limit. An appropriate lower-force limit was established using Equation 2 with a posture of 15˚ abduction and 30˚ flexion and the small female stature (150 cm) to determine the force associated with each level of hip injury risk. The lower-force limit was then determined by multiplying this factor by 1.4 (the scale factor between peak force at the human hip and peak force at the Hybrid III femur load cell for the midsize male for knee loading by a force-limiting knee bolster).

Like the upper-force limit, the transition impulse for the small female injury assessment criteria was also developed by scaling midsize male data. For impulse, the scaling factor was 0.580. This factor was derived as described in the Appendix, using the same dimensional analysis based scaling techniques described by Mertz et al. (2003). Scaling the transition impulse also requires scaling the method used to calculate impulse. For the KTH injury assessment criteria for the Hybrid III midsize male, impulse is calculated by integrating the femur force history from the start of knee loading to the time that force last exceeds 4.05 kN. For the small-female ATD, impulse is calculated by integrating the femur force history from the start of knee loading to the time that force last exceeds 2.75 kN, which is equal to 4.05 kN multiplied by the 0.679 femur force scaling factor reported by Mertz et al. (2003).

Table 6 lists the small female injury assessment criteria for levels of KTH injury risk ranging from 3% to 75%. Transition impulse and the lower-force limit for the 3% and 5% injury assessment reference boundaries do not apply with this ATD since the upper-force limit is less than the lower-force limit and therefore applies to all femur force histories. These injury assessment reference boundaries individually assess whether a particular Hybrid III small female femur force history is associated with a risk of injury greater than a specified value. Alternatively, these boundaries can be used together, as described above, to assess the maximum possible risk of hip injury and the risk of knee/distal femur injury associated with a particular femur force history.

Table 6. Injury Assessment Criteria Associated with Risk of KTH Injury from 3% to 75% for Hybrid III Small-Female ATD.

Risk (%)	Lower-force limit (kN)	Transition impulse (Ns)	Upper-force limit (kN)
3	3.65*	NA*	3.37
5	3.82*	NA*	3.86
10	4.13	70.6	4.66
15	4.33	74.1	5.22
20	4.49	77.0	5.67
25	4.65	79.5	6.06
30	4.79	81.9	6.41
35	4.91	84.4	6.74
40	5.05	86.6	7.04
45	5.18	88.9	7.34
50	5.33	91.2	7.62
75	6.09	104.8	9.14

*Not applicable because the upper and lower-force limits are equal.

DISCUSSION

The injury assessment reference boundaries listed in Table 5 were computed such that, under the assumptions of the model, all combinations of peak Hybrid III femur force and impulse that are associated with a risk of KTH injury that is greater than a specified percentage will be above the boundary. However, some combinations of peak femur force and impulse that are associated with risks of injury that are less than the value associated with the boundary can fall above the boundary. In other words, each boundary represents a test with approximately 100% sensitivity but less than 100% specificity for peak forces between the upper and lower-force limits. For peak femur forces that are less than the lower-force limit or greater than the upper-force limit, the injury assessment reference boundary will accurately predict injury risk, subject to the limitations discussed below.

Because they were developed using one-dimensional lumped parameter models, the injury assessment reference boundaries listed in Tables 5 and 6 are limited in several ways. First, the models and the IARVs only apply to symmetric knee loading. The farther a knee-loading condition deviates from applying similar forces to both knees, the less applicable these IARVs will be. This is because asymmetric knee loading has the potential to increase the amount mass behind the hip on the side to which higher force is being applied. This will increase the percentage of force applied to the knee transmitted to the hip and thereby increase the risk of hip injury in a manner that is not accounted for by the lower force limits described in this paper. As a result, the new injury assessment criteria described in this paper will under predict hip-injury risk for asymmetric knee loading. However, this limitation is not important for frontal crash testing in FMVSS 208 and NCAP, where loading is primarily symmetric.

In addition, because the injury assessment reference boundaries were developed using one-dimensional models, they cannot predict two-dimensional phenomena, such as femur bending, which is thought to be the primary mechanism of femoral shaft fracture in frontal crashes (Viano and Stalnaker, 1980). However, since most femur bending in frontal crashes is produced by axial compression (which is assessed by the injury reference boundaries), the failure of the injury assessment reference boundaries to account for femur bending may not be a major limitation.

The models also do not account for the effects of lower-extremity muscle tension due to occupant braking and/or bracing on KTH injuries. Based on the results of recent FE modeling, muscle activation reduces the percentage of force applied to the human knee that is transmitted to the hip by increasing the coupling of muscle mass distal to the hip (Chang, 2009). As a result, with muscle activation, the ratio of peak force at the Hybrid III femur load cell to peak force at the cadaver hip used to establish the lower force limit of the new IARVs will be greater, and the ATD femur forces associated with the lower bound will also be greater.

The injury assessment reference boundaries listed in Tables 5 and 6 are all associated with a single hip posture, which is considered typical of a midsize male at the time of peak knee-bolster loading. Variations from this posture will affect hip-injury tolerance, and will therefore shift the lower force limit and the transition impulse, but will have no effect on the upper force limit associated with knee/distal-femur fracture, which is posture independent.

The injury assessment reference boundaries developed in this study are based on limiting the risks of hip and knee/distal-femur injuries to the same risk levels. However, hip injuries are generally considered more costly to society, more difficult to treat, and more disabling than knee or distal femur injuries (Read et al. 2002). Therefore, in the future, it may be appropriate to calculate the new injury assessment criteria using lower risks of hip injury than the risks of knee/distal-femur injury.

The new KTH injury assessment criterion developed in this study were tested to ensure that they appropriately identify loading conditions that are associated with risks of KTH injury greater than specified levels. Further evaluation of the new injury criterion is described in a companion paper (Kirk and Kuppa 2009), which applies the injury assessment reference boundaries to Hybrid III femur forces measured in NHTSA and IIHS crash tests, and compares the predicted levels of injury risk to those observed in similar real-world crashes investigated in the National Automotive Sampling Systems (NASS).

Developing KTH injury assessment criteria for ATDs would be greatly simplified if the Hybrid III family of dummies produced similar knee impact forces and transmitted similar amounts of force to the hip as the humans that they are designed to represent. With improved ATD biofidelity, the risks of KTH injury could be assessed by applying peak forces measured by ATD femur and acetabular load cells to existing injury risk curves for the femur and hip, respectively. However, with current ATDs, the modeling approach described in this paper is needed to accurately interpret ATD femur forces with respect to human injury risk.

CONCLUSIONS

A one-dimensional lumped-parameter model of the midsize-male Hybrid III ATD has been developed and validated. Simulations with this model and the previously described lumped-parameter model of the midsized male cadaver were performed to explore the relationship between forces in the Hybrid III KTH complex and forces in the human KTH complex. Results of these simulations indicate that the relationships between peak forces measured by the Hybrid III femur load cell and peak forces in the cadaver KTH complex vary with the force-deflection characteristics of the knee bolster. Since knee bolster characteristics in different vehicles vary, it is not possible to develop a singular relationship between peak forces measured by the Hybrid III femur load cell and the risks of injury to the human KTH complex.

For this reason, a new injury assessment criteria for the KTH was developed that uses peak Hybrid III femur force and the impulse of Hybrid III femur force to define the smallest possible femur force histories that are associated with a given probability of KTH injury. The use of impulse allows the new injury assessment criteria to identify the high-rate, short-duration loading associated with knee/distal-femur fractures and the lower-rate, longer-duration loading conditions associated with hip fractures.

ACKNOWLEDGEMENTS

This research was sponsored by the National Highway Traffic Safety Administration, U.S. Department of Transportation under contract DTNH22-05-H-01020.

REFERENCES

Chang, C.Y. (2009). The effects of muscle forces on the predicted risk of knee-thigh-hip injury in frontal crashes. Ph.D. Dissertation. The University of Michigan, Ann Arbor, MI

Chang, C.Y. Rupp, J.D., Schneider, L.W., and Kikuchi, N. (2008). Development of a Finite Element Model to Study the Effects of Muscle Forces on Knee-Thigh-Hip Injuries in Frontal Crashes. Stapp Car Crash Journal 52.

Donnelly, B.R. and Roberts, D.P. (1987). Comparison of cadaver and Hybrid III dummy response to axial impacts of the femur. Proceedings of the Thirty-First Stapp Car Crash Conference, Paper No. 872204, pp. 105-116. Society of Automotive Engineers, Warrendale, PA.

Kirk K. and Kuppa, S. (2009). Application and Evaluation of a Novel KTH Injury Criterion for the Hybrid III Dummy in Frontal Crash Test Environments. Paper #09-0196. Proceedings of the 21st International Technical Conference on the Enhances Safety of Vehicles. National Highway Traffic Safety Association, Washington DC.

Kuppa, S., Wang, J., Haffner, M., and Eppinger, R. (2001). Lower extremity injuries and associated injury criteria. Proceedings of the 17th International Technical Conference on the Enhanced Safety of Vehicles, Paper No. 457. National Highway Traffic Safety Association, Washington, DC.

Kuppa, S. and Fessahaie, O. (2003). An overview of knee-thigh-hip injuries in frontal crashes in the United States. Proceedings of the 18th International Technical Conference on Experimental Safety Vehicles. National Highway Traffic Safety Association, Washington DC.

Masson and Cavallero (2003). Comparison between Hybrid III Dummy and Cadaver knee response in frontal impact. Proceedings of the 2003 International Conference on the Biomechanics of Impact, pp 359-360. IRCOBI, Bron, France.

Read, K. M., Burgess, A. R., Dischinger, P. C., Kufera, J. A., Kerns, T. J., Ho, S. M., and Burch, C. (2002). Psychosocial and physical factors associated with lower extremity injury. Proceedings of the 46th Annual Conference of the Association for the Advancement of Automotive Medicine, pp. 289-303. Association for the Advancement of Automotive Medicine. Des Plaines, IL

Rupp, J.D., Reed M.P., Jeffreys, T.J., and Schneider L.W (2003a). Effects of hip posture on the frontal impact tolerance of the human hip joint. Stapp Car Crash Journal 47: 21-33.

Rupp, J.D., Reed, M.P., Madura, N.H., Kuppa, S., and Schneider L.W. (2003b) Comparison of knee/femur force-deflection response of the Thor, Hybrid III, and human cadaver to dynamic frontal-impact knee loading. Proceedings of the 18th International Conference of Experimental Safety Vehicles. National Highway Traffic Safety Administration, Washington DC.

Rupp, J.D. (2006). Biomechanics of hip fractures in frontal motor-vehicle crashes. Ph.D. Dissertation. The University of Michigan, Ann Arbor, MI.

Rupp J.D., Reed, M.P., Madura, N.H., Miller, C.S., Kuppa, S.M., and Schneider L.W. (2005). Comparison of the inertial response of the THOR-NT, Hybrid III, and unembalmed cadaver to simulated knee-to-knee-bolster impacts. Proceedings of the 19th International Technical Conference on the Enhanced Safety of Vehicles, Paper 05-0086. National Highway Traffic Safety Administration, Washington, DC.

Rupp, J.D., Miller, C.S., Madura, N.H., Reed, M.P., and Schneider L.W. (2007) Characterization of knee impacts in frontal crashes. Proceedings of the 20th International Technical Conference on the Enhanced Safety of Vehicles. Paper 07-0345. National Highway Traffic Safety Administration, Washington DC.

Rupp, J.D., Miller, C.S., Madura, N.H., Reed, M.P., Klinich, K.D., and Schneider L.W. (2008a). Characterization of Knee-Thigh-Hip Response in Frontal Impacts Using Biomechanical Testing and Computational Simulation. Stapp Car Crash Journal 52

Rupp, J.D. and Flannagan C.A. (2009). Development of New Injury Risk Curves for the Knee/Distal and Hip for Use in Frontal Impact. Report # UMTRI-2009-08, University of Michigan Transportation Research Institute, Ann Arbor, MI.

Society of Automotive Engineers Dummy Testing Equipment Subcommittee (1998). User's manual for the midsize Hybrid III test dummy, Engineering Aid 23. Society of Automotive Engineers, Warrendale, PA.

Viano, D.C. and Stalnaker, R.L. (1980). Mechanisms of femoral fracture. Journal of Biomechanics 13: 701-715.

APPENDIX: DERIVATION OF IMPULSE SCALING FACTOR

Since the units of impulse are Ns, the scale factor for impulse, λ_I, must equal the scale factor for force, λ_F, multiplied by the scale factor for time, λ_{Time}, as shown in Equation A1. The scale factor for force is defined by Equation A2 (Mertz et al. 2003). The scale factor for time was derived by recognizing that the units of force are kg m/s^2 and that as a result, the scale factor for force must equal the scale factor for mass, λ_m, multiplied by the scale factor for width/height, λ_x, divided by the square of the scale factor for time (Equation A3). Since this quantity is equal to the scale factor for force (λ_x^2), it follows that the scale factor for time is defined by Equation A4. Substituting Equation A4 into Equation A1 gives the formula scale factor for impulse that is listed in Equation A5. Applying the values for λ_F, λ_m, and λ_x reported by Mertz et al., which are 0.679, 0.601, and 0.824, respectively, to Equation A5 gives a scale factor for impulse of 0.580.

$$\lambda_I = \lambda_F * \lambda_{Time} \quad [A1]$$

From Mertz et al. (2003), $\lambda_F = \lambda_x^2$ [A2]

Since the units of force are kg m /s^2,

$$\lambda_F = \lambda_m * \lambda_x / \lambda_{Time}^2 = \lambda_x^2 \quad [A3]$$

$$\lambda_{Time} = [\lambda_m / \lambda_x]^{0.5} \quad [A4]$$

$$\lambda_I = \lambda_F * [\lambda_m / \lambda_x]^{0.5} \quad [A5]$$